JOURNAL OF GEOPHYSICAL RESEARCH, VOL. 88, NO. C10, PAGES 6043–6051, JULY 20, 1983

On the Dynamics of the Ice Sheets 2

P. HALFAR[1]

Max-Planck-Institut für Meteorologie, Hamburg, Federal Republic of Germany

The equation which describes the motion of an ice sheet under its own weight has a cylindrically symmetric similarity solution. The initial value problem of the equation of motion which has been linearized in the deviations from this similarity solution is solved by an expansion of the solution in terms of eigenfunctions of the linearized equation. The linearized equation determines, for all ice sheets of the same volume, an asymptotically stable motion. These results are compared with the corresponding results of the two-dimensional case (Halfar, 1981).

THE SIMILARITY SOLUTION

This paper is an extension of *Halfar*'s [1981] two-dimensional analysis to the three-dimensional case. A homogeneous ice sheet is considered, which is frozen to a flat, horizontal bed, moves under its own weight according to Glen's flow law, and is not governed by other influences. A motion by shear strain parallel to the bed is assumed, changes of the shear stress in horizontal direction are neglected in comparison with changes of the pressure in vertical direction, and changes of the vertical velocity in horizontal direction are neglected in comparison with changes of the horizontal velocity in vertical direction.

The position of the ice surface is described by its height h at times t above the bed point with Cartesian coordinates x, y and cylindrical coordinates ρ, ϕ, where h, x, y, ρ, and t are dimensionless coordinates with L and T as units of length and time, respectively [*Halfar*, 1981]. The corresponding equation of motion [*Mahaffy*, 1976],

$$\frac{\partial h}{\partial t} = \nabla(\nabla h\, |\nabla h|^{n-1}\, h^{n+2}) \tag{1}$$

for the time evolution of the ice surface has a cylindrically symmetric (three-dimensional case) similarity solution which is compared with the two-dimensional solution [*Halfar*, 1981]:

Three-dimensional case

$$h = (aV)^{1/3} f^2(t) g(\eta) \tag{2}$$

where

$$\eta = \rho f(t)(aV)^{-1/3} \tag{3}$$

$$g(\eta) = (1 - \eta^{(n+1)/n})^{n/(2n+1)} \tag{4}$$

$$f(t) = \left(\frac{t}{\tau}\right)^{-1/(5n+3)} \tag{5}$$

$$\tau = \frac{1}{(5n+3)} \left(\frac{2n+1}{n+1}\right)^n (aV)^{-n/3} \tag{6}$$

$$a = \frac{(n+1)}{2\pi n} \Gamma\left(\frac{7n^2+6n+1}{(n+1)(2n+1)}\right) \Gamma^{-1}\left(\frac{2n}{n+1}\right) \Gamma^{-1}\left(\frac{3n+1}{2n+1}\right) \tag{7}$$

Two-dimensional case

$$h = (aV)^{1/2} f(t) g(\eta) \tag{8}$$

where

$$\eta = x f(t)(aV)^{-1/2} \tag{9}$$

$$g(\eta) = (1 - |\eta|^{(n+1)/n})^{n/(2n+1)} \tag{10}$$

$$f(t) = \left(\frac{t}{\tau}\right)^{-1/(3n+2)} \tag{11}$$

$$\tau = \frac{1}{(3n+2)} \left(\frac{2n+1}{n+1}\right)^n (aV)^{-n/2} \tag{12}$$

$$a = \frac{(n+1)}{2n} \Gamma\left(\frac{5n^2+5n+1}{(n+1)(2n+1)}\right) \Gamma^{-1}\left(\frac{n}{n+1}\right) \Gamma^{-1}\left(\frac{3n+1}{2n+1}\right) \tag{13}$$

In both cases, V denotes the total volume measured in units of L^3 or L^2, as appropriate, n the exponent in Glen's flow law, and Γ the Γ function.

The time evolution of the maximal height H and the half-width R can be obtained from (2) with (3) and (8) with (9), respectively:

Three-dimensional case

$$H(t) = h|_{\eta=0} = (aV)^{1/3} f^2(t) \tag{14}$$

$$R(t) = \rho|_{\eta=1} = (aV)^{1/3} f^{-1}(t) \tag{15}$$

Two-dimensional case

$$H(t) = h|_{\eta=0} = (aV)^{1/2} f(t) \tag{16}$$

$$R(t) = x|_{\eta=1} = (aV)^{1/2} f^{-1}(t) \tag{17}$$

The total volume,

Three-dimensional case

$$V = \frac{H(t) R^2(t)}{a} \tag{18}$$

Two-dimensional case

$$V = \frac{H(t) R(t)}{a} \tag{19}$$

is conserved.

In both cases, (4) and (10), the same rescaled surface profile of the ice sheet in a plane perpendicular to the bed and to the ice edge is obtained. The half-widths, (15) and (17), are power functions of the time t with power exponent $1/(5n+3)$ and $1/(3n+2)$, respectively.

[1] Now at Leitselle Umweltschutz, Hamburg, Federal Republic of Germany.

Paper number 3C0340.
0148-0227/83/003W-0340$05.00

THE PERFECT PLASTICITY LIMIT

In the following it is shown how Orowan's solution can be obtained from the similarity solution in the perfect plasticity limit $n \to \infty$. In this limit the ice sheets are described as well in the two-dimensional as in the cylindrically symmetric three-dimensional case by Orowan's solution [*Nye*, 1952] which is determined by its parabolic surface profile and the relation [*Weertman*, 1964]

$$\frac{2\tau_0 \hat{R}}{\rho g \hat{H}^2} = 1 \tag{20}$$

between its dimensional half-width $\hat{R}$ and dimensional maximal height $\hat{H}$, where ρ is the density of the ice, g the acceleration of gravity, and the stress τ_0 is a parameter in Glen's flow law, which occurs in two forms in the literature [*Nye*, 1957; *Weertman*, 1964]:

$$\dot{\varepsilon} = \left(\frac{\tau}{A}\right)^n = C\left(\frac{\tau}{\tau_0}\right)^n \tag{21}$$

with

$$A^n = C^{-1}{\tau_0}^n \tag{22}$$

where $\dot{\varepsilon}$ and τ denote the second invariants of the strain rate and the deviatoric stress tensor, respectively.

In the three-dimensional and two-dimensional cases the rescaled surface profiles, (4) and (10), respectively, become parabolic in the perfect plasticity limit:

Three-dimensional case

$$g_\infty(\eta) = \lim_{n\to\infty} g(\eta) = (1-\eta)^{1/2} \tag{23}$$

Two-dimensional case

$$g_\infty(\eta) = \lim_{n\to\infty} g(\eta) = (1-|\eta|)^{1/2} \tag{24}$$

The second property, (20), is derived in a way which is different from that of *Halfar* [1981]. The time which a similarity solution of volume V needs to extend from half-width 0 to half-width R is given by (cf. (5), (6), and (15) or (11), (12), and (17))

Three-dimensional case

$$t = \frac{1}{(5n+3)}\left(\frac{2n+1}{n+1}\right)^n \frac{R^{5n+3}}{(aV)^{2n+1}} \tag{25}$$

Two-dimensional case

$$t = \frac{1}{(3n+2)}\left(\frac{2n+1}{n+1}\right)^n \frac{R^{3n+2}}{(aV)^{2n+1}} \tag{26}$$

Reintroducing the dimensional time $\hat{t}$, half-width $\hat{R}$, and height $\hat{H}$ by [cf. *Halfar*, 1981]

$$\hat{t} = tT \qquad \hat{R} = RL \qquad \hat{H} = HL \tag{27}$$

and using (18), (22), and (25) or (19), (22), and (26), as appropriate, yields

Three-dimensional case

$$\hat{t} = \frac{1}{C}\left(\frac{2\tau_0}{\rho g}\frac{\hat{R}}{\hat{H}^2}\right)^n \frac{\hat{R}}{\hat{H}} \frac{(n+2)}{2(5n+3)}\left(\frac{2n+1}{2n+2}\right)^n \tag{28}$$

Two-dimensional case

$$\hat{t} = \frac{1}{C}\left(\frac{2\tau_0}{\rho g}\frac{\hat{R}}{\hat{H}^2}\right)^n \frac{\hat{R}}{\hat{H}} \frac{(n+2)}{2(3n+2)}\left(\frac{2n+1}{2n+2}\right)^n \tag{29}$$

as dimensional time which a similarity solution needs to extend from a δ function distribution with half-width 0 to a distribution with dimensional half-width $\hat{R}$ and dimensional maximal height $\hat{H}$. In the three-dimensional case this time is smaller than in the two-dimensional case by a factor of $(3n+2)/(5n+3)$ which is equal to 11/18 in the typical case $n = 3$.

In the limit $n \to \infty$, the shallow profiles, i.e., $2\tau_0\hat{R}/\rho g\hat{H}^2 > 1$, are never reached by an extending similarity solution as $\hat{t} \to \infty$, and the steep profiles, i.e., $2\tau_0\hat{R}/\rho g\hat{H}^2 < 1$, are reached instantaneously as $\hat{t} \to 0$. Therefore the profiles with (20) are the only ones which can exist under these circumstances.

THE SOLUTION OF THE LINEARIZED RESCALED EQUATION OF MOTION

Applying the time-dependent rescalings which transformed the similarity solution of volume V to the time-independent solution $g(\eta)$, (4) or (10), to the general solution h of (1) yields the rescaled general solution G:

Three-dimensional case

$$G(t, \eta, \phi) = (aV)^{-1/3} f^{-2}(t) h \tag{30}$$

Two-dimensional case

$$G(t, \eta) = (aV)^{-1/2} f^{-1}(t) h \tag{31}$$

where $a, f(t)$, and η are given by (7), (5), and (3) or (13), (11), and (9).

The deviation of the rescaled solution G from the rescaled similarity solution g is described by the function ε defined through

Three-dimensional case

$$\eta = (1 + \varepsilon(t, \xi, \phi))\xi \tag{32}$$

$$G(t, \eta, \phi) = (1 + \varepsilon(t, \xi, \phi))g(\xi) \tag{33}$$

Two-dimensional case [*Halfar*, 1981]

$$\eta = (1 + \varepsilon(t, \xi))\xi \tag{34}$$

$$G(t, \eta) = (1 + \varepsilon(t, \xi))g(\xi) \tag{35}$$

In the three-dimensional case the deviation ε is not assumed to be cylindrically symmetric and thus depends also on the angular variable ϕ.

Inserting (3), (30), (32), and (33) or (9), (31), (34), and (35) in the equation of motion (1) and expanding up to first order in ε yields the linearized rescaled equation of motion

$$t\frac{\partial \varepsilon}{\partial t} = \mathscr{L}\varepsilon \tag{36}$$

where $\partial/\partial t$ denotes differentiation with fixed ξ and $\mathscr{L}$ is a linear differential operator in ξ and ϕ or in ξ (cf. Appendix A or *Halfar* [1981]).

In the three-dimensional case as well as in the two-dimensional case the condition

$$\left|\frac{\partial}{\partial \xi}(\xi\varepsilon)\right| < 1 \tag{37}$$

guarantees the regularity of the transformations (32) and (33) or (34) and (35) (cf. Appendix A or *Halfar* [1981]) and is equivalent to the physical boundary condition of vanishing ice flux $\mathbf{q}$ at the glacier edge (cf. Appendix C):

$$\mathbf{q}|_{\text{edge}} = -\nabla h\, |\nabla h|^{n-1}\, h^{n+2}|_{\text{edge}} = 0 \tag{38}$$

The proof of this equivalence for the two-dimensional case was not given by *Halfar* [1981] but can be carried out in a manner similar to that shown in Appendix C.

The eigenvalues $\mu_{m,k}$ and normalized eigenfunctions $\varepsilon_{m,k}(\xi, \phi)$ or $\varepsilon_{m,k}(\xi)$ of the operator $\mathscr{L}$ in (36) satisfying the boundary condition (38) have the mode numbers

Three-dimensional case

$$m = \cdots -1, 0, 1 \cdots \qquad k = 0, 1, 2, \cdots \tag{39}$$

Two-dimensional case

$$m = 0, 1 \qquad k = 0, 1, 2, \cdots \tag{40}$$

where in the two-dimensional case, $m = 0$ denotes the symmetric case and $m = 1$ the antisymmetric case [*Halfar*, 1981]. They are given by

Three-dimensional case (cf. Appendix B)

$$\mu_{m,k} = \frac{-1}{(5n+3)}\left(\frac{(1-n)}{2} + (n+1)k + \frac{(n+1)(2n+1)}{n}k^2\right) - \frac{1}{(5n+3)}\left(\frac{(2n+1)}{n}k + \frac{1}{2}\right)((n-1)^2 + 4nm^2)^{1/2} \tag{41}$$

$$\varepsilon_{m,k}(\xi, \phi) = e^{im\phi}u_{m,k}(z)f_m(z) \tag{42}$$

where

$$z = \xi^{(n+1)/n} \tag{43}$$

$$f_m(z) = \left(1 - \frac{nz}{(2n+1)}\right)^{-1} \cdot \exp\left[\frac{\ln z}{2(n+1)}(-n + 1 + ((n-1)^2 + 4nm^2)^{1/2})\right] \tag{44}$$

$$u_{m,k}(z) = h_{m,k}{}^{-1/2}G_k(p_m, q_m, z) \tag{45}$$

$$p_m = \frac{n}{(2n+1)} + \frac{1}{(n+1)}((n-1)^2 + 4nm^2)^{1/2} \tag{46}$$

$$q_m = 1 + \frac{1}{(n+1)}((n-1)^2 + 4nm^2)^{1/2} \tag{47}$$

$$h_{m,k} = \frac{k!\Gamma(k+q_m)\Gamma(k+p_m)\Gamma(k+p_m-q_m+1)}{(2k+p_m)\Gamma^2(2k+p_m)} \tag{48}$$

Two-dimensional case [*Halfar*, 1981]

$$\mu_{m,k} = -\frac{(n+1)(2n+1)}{n(3n+2)}\left(k + \frac{m}{(n+1)}\right) \cdot \left(k + \frac{m}{(n+1)} + \frac{(n^2-n-1)}{(n+1)(2n+1)}\right) \tag{49}$$

$$\varepsilon_{m,k}(\xi) = \left(\frac{\xi}{|\xi|}\right)^m u_{m,k}(z)f_m(z) \tag{50}$$

where

$$z = |\xi|^{(n+1)/n} \tag{51}$$

$$f_m(z) = \left(1 - \frac{nz}{(2n+1)}\right)^{-1} \cdot \exp\left[\frac{\ln z}{2(n+1)}(-n + 1 + ((n-1)^2 + 4nm^2)^{1/2})\right] \tag{52}$$

$$u_{m,k}(z) = h_{m,k}{}^{-1/2}G_k(p_m, q_m, z) \tag{53}$$

$$p_m = \frac{n^2-n-1}{(n+1)(2n+1)} + \frac{2(2n+1)m}{(n+1)(2n+1)} \tag{54}$$

$$q_m = \frac{n}{(n+1)} + \frac{2m}{(n+1)} \tag{55}$$

$$h_{m,k} = \frac{k!\Gamma(k+q_m)\Gamma(k+p_m)\Gamma(k+p_m-q_m+1)}{(2k+p_m)\Gamma^2(2k+p_m)} \tag{56}$$

The function $G_k(p_m, q_m, z)$ denotes the Jacobi polynomial which is proportional to the hypergeometric function $F(-k, k+p_m, q_m; z)$. The properties of the special functions in this section are described by *Abramowitz and Stegun* [1970].

Expanding ε in terms of eigenfunctions (42) or (50),

Three-dimensional case

$$\varepsilon(t, \xi, \phi) = \sum_{m=-\infty}^{m=+\infty}\sum_{k=0}^{k=\infty} a_{m,k}(t)\varepsilon_{m,k}(\xi, \phi) \tag{57}$$

Two-dimensional case

$$\varepsilon(t, \xi) = \sum_{m=0}^{m=1}\sum_{k=0}^{k=\infty} a_{m,k}(t)\varepsilon_{m,k}(\xi) \tag{58}$$

inserting (57) or (58) in (36), and comparing the coefficients of every eigenfunction separately yields

$$t\dot{a}_{m,k}(t) = \mu_{m,k}a_{m,k}(t) \tag{59}$$

as differential equation for the time evolution of the amplitude $a_{m,k}(t)$ with the solution

$$a_{m,k}(t) = \left(\frac{t}{t_0}\right)^{\mu_{m,k}} a_{m,k}(t_0) \tag{60}$$

The equations (57) or (58) and (60) solve the initial value problem for the linearized rescaled equation of motion (36) under the boundary condition of vanishing ice flux (38). The orthogonality relations for the functions (45) or (53) and the inverse relation to (57) or (58) are given in Appendix D.

For the three-dimensional case the radial dependences in the directions $\phi = 0$ (positive abscissa) and $\phi = \pi$ (negative abscissa) of rescaled surface profiles belonging to some of the eigenfunctions $\varepsilon_{m,k}$ (42) are displayed in Figure 1 for the case $n = 3$. The profiles with $m = 0$ and $m = \pm 1$ look very similar to the symmetric or antisymmetric profiles in the two-dimensional case [*Halfar*, 1981]. The profiles with $(m, k) = (0, 0), (\pm 1, 0), (0, 1)$ can be generated from the similarity solution by infinitesimal shifts in volume, two orthogonal horizontal directions, and time, respectively, and therefore correspond to the profiles $(m, k) = (0, 0), (1, 0), (0, 1)$ in the two-dimensional case (cf. discussion and *Halfar* [1981]).

The singularities of the surface slopes occurring at the center of the ice sheet in the cases $m = 1$ and $m = 2$ or in the case $m = 1$ (antisymmetric case, cf. *Halfar* [1981]), which are determined by the functions $f_m(z)$ in (44) or (52), are due to the nonlinear behavior of the flux $\mathbf{q}$ (cf. (38)) in ∇h and indeed disappear in the case $n = 1$ when the flux becomes linear in ∇h. In the three-dimensional case the angular dependence of the eigenfunctions (42) is given by $e^{im\phi}$.

DISCUSSION

In the three-dimensional case as well as in the two-dimensional case, all eigenvalues (41) or (49) except the first, $\mu_{0,0}$, are negative, and therefore $\varepsilon \to 0$ for $t \to \infty$ if $a_{0,0} \equiv 0$ (cf. (57) or (58) and (60)), i.e., the similarity solution is asymptotically stable under all perturbations of its initial value data

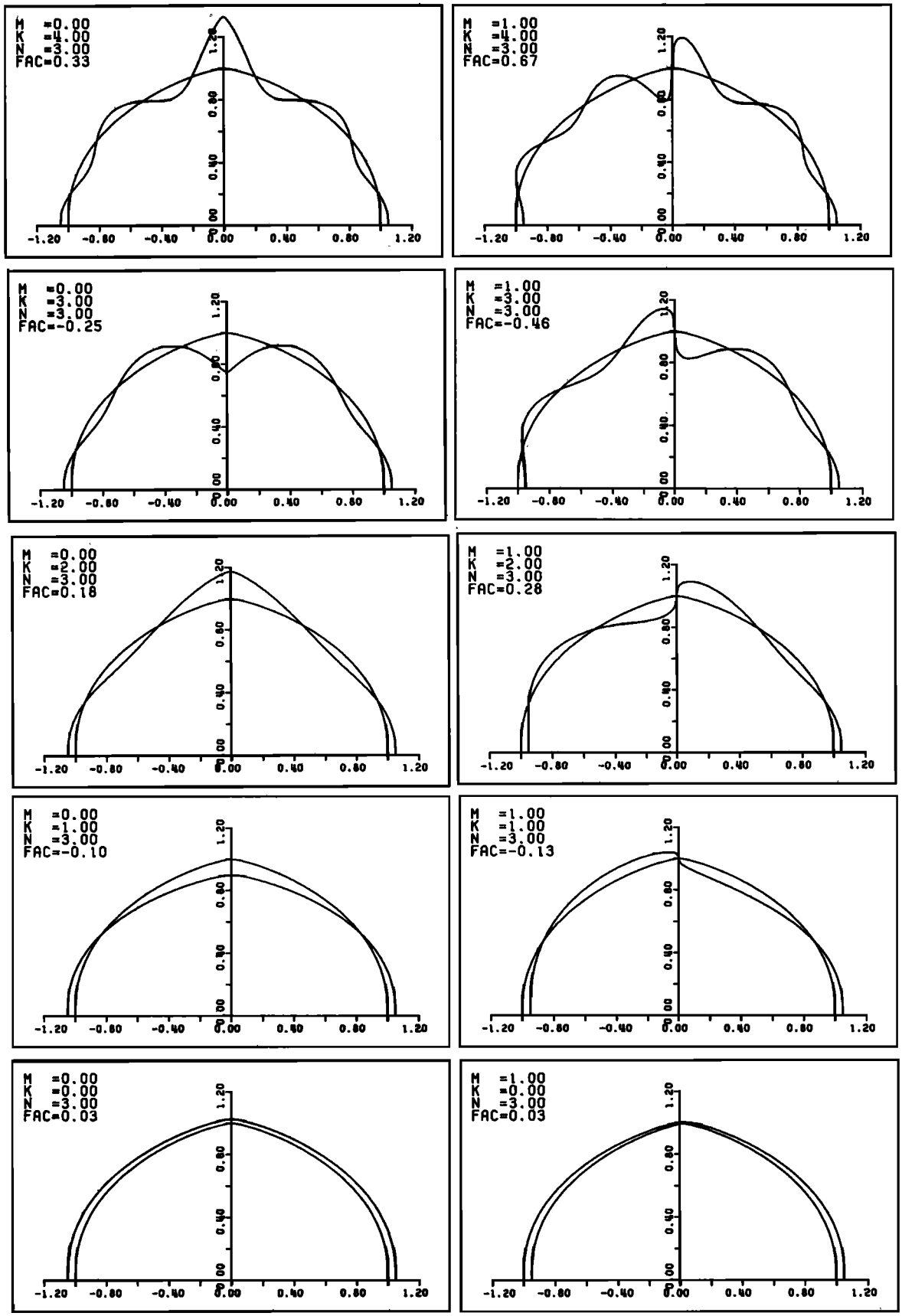

Fig. 1. Each picture shows the radial dependence $g(\eta)$ versus η of the rescaled cylindrically symmetric similarity solution (4) which is obtained from the similarity solution (2) by time-dependent rescalings of the distance ρ from the origin and of the height h, such that it becomes time-independent, extends from $\eta = 0$ to $\eta = 1$ in radial direction, and has maximal height $g(0) = 1$. The radial dependence $(1 + c_{m,k}\varepsilon_{m,k}(\xi, 0))g(\xi)$ versus $(1 + c_{m,k}\varepsilon_{m,k}(\xi, 0))\xi = \eta$ (cf. (32), (33)) in the direction $\phi = 0$ of the occuring rescaled surface profiles represent deviations from the similarity solution belonging to eigenfunctions $c_{m,k}\varepsilon_{m,k}$ (cf. (42)) of (36) where $m\,(=M) = 0 \cdots \pm 3$ denotes the angular and $k\,(=K) = 0 \cdots 4$ the radial mode number. The constants $c_{m,k}$ have been chosen such that all occuring deviations have the same order of magnitude. The negative part of the abscissa corresponds to the direction $\phi = \pi$. The value $n = 3$ has been chosen for the exponent in Glen's flow law.

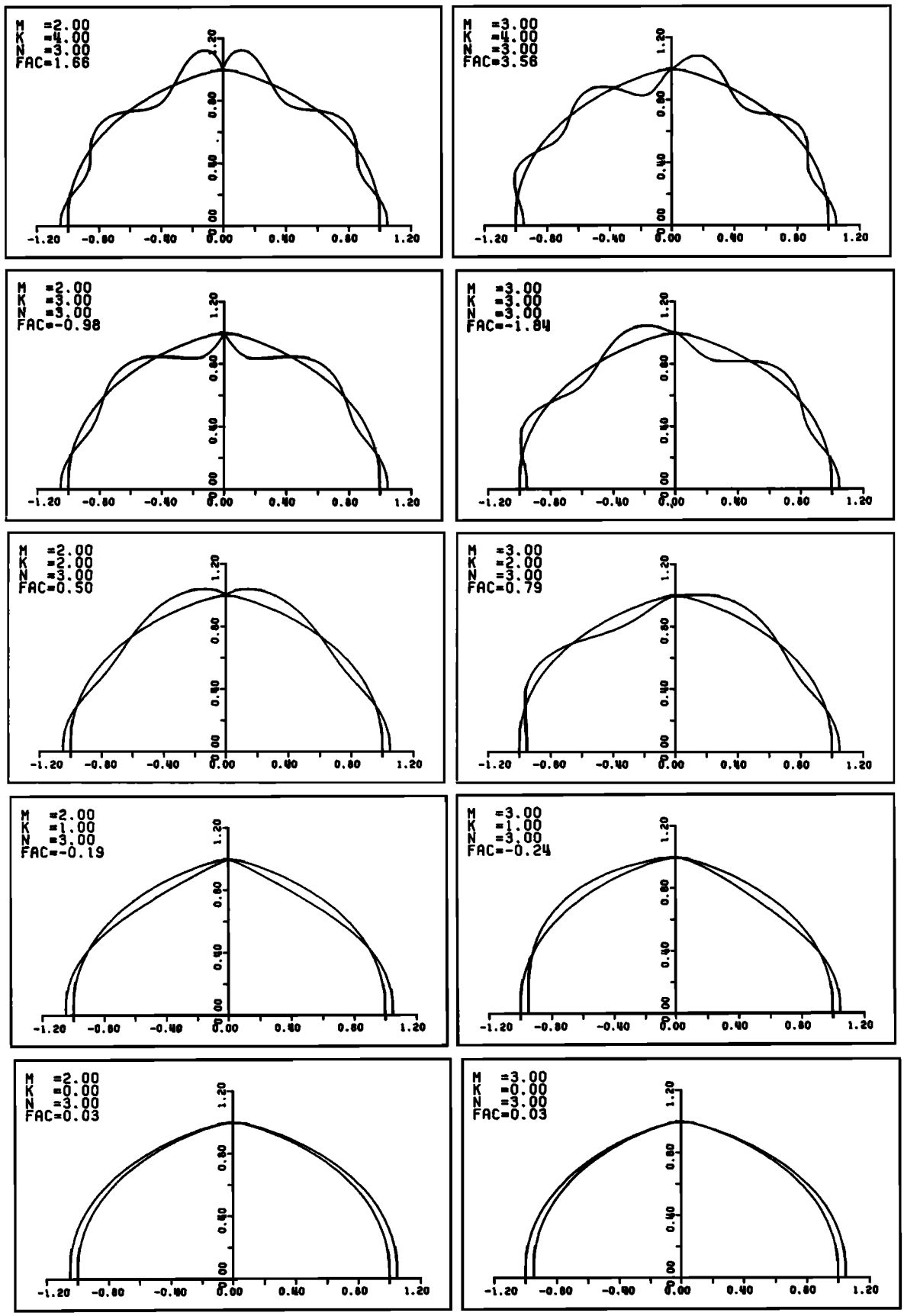

Fig. 1. (continued)

which leave the volume invariant. In the two-dimensional case the three modes with mode numbers $(m, k) = (0, 0), (1, 0), (0, 1)$ can be generated from the similarity solution by shifts in volume, space, and time, respectively [*Halfar*, 1981]. In the three-dimensional case, two linearly independent shifts in horizontal directions are possible, and thus four modes with $(m, k) = (0, 0), (\pm 1, 0), (0, 1)$ can be generated by shifts in volume, space, and time in the following way. The four parameters of the similarity solution are its volume V, the xy coordinates x_0, y_0 of its center of mass, and the initial time t_0 at which the similarity solution is a δ function distribution in space (do not confuse this t_0 with the time t_0 in the solution (60) of the initial value problem for the linearized equation). The solution (2) belongs to the value $x_0 = y_0 = t_0 = 0$. Representing the deviation of the similarity solution which belongs to the parameters $V + \delta V$, x_0, y_0, t_0 from the solution (2) by a function $\varepsilon(t, \xi, \phi)$ according to (30), (32), (33) and differentiating this function at arbitrary, fixed time with respect to δV, x_0, y_0, t_0 at $\delta V = x_0 = y_0 = t_0 = 0$ yields four eigenfunctions of (36) which are, up to constant factors equal to $\varepsilon_{0,0}(\xi, \phi)$, the real and imaginary part of $\varepsilon_{1,0}(\xi, \phi) = \bar{\varepsilon}_{-1,0}(\xi, \phi)$ and $\varepsilon_{0,1}(\xi, \phi)$, respectively.

The relative decrease $-da_{m,k}/a_{m,k}$ of the amplitude $a_{m,k}$ during the time evolution measured in units dR/R which is the relative increase of the cap's half-width is given by

Three-dimensional case (cf. (59), (15), (5))

$$-\frac{R(t)}{a_{m,k}(t)}\frac{da_{m,k}(t)}{dR(t)} = -(5n + 3)\mu_{m,k} \tag{61}$$

Two-dimensional case [*Halfar*, 1981]

$$-\frac{R(t)}{a_{m,k}(t)}\frac{da_{m,k}(t)}{dR(t)} = -(3n + 2)\mu_{m,k} \tag{62}$$

The lowest of these values for $n = 3$ are given by

Three-dimensional case (61)

↑ k	1 0	18 0	1	2.6	4.3	6	7.7	9.4	11.2	12.9	14.6	16.3	18.1
	$m\rightarrow$	0	±1	±2	±3	±4	±5	±6	±7	±8	±9	±10	±11

Two-dimensional case (62) [*Halfar*, 1981]

↑ k	1 0	11 0	1
	$m\rightarrow$	0	1

For the modes (m, k) which are generated by shifts in volume $(m = 0, k = 0)$ and space $(m = \pm 1$ or $1, k = 0)$ the occurring values are equal to 0 and 1 in the three-dimensional as well as in the two-dimensional case. The mode $(m, k) = (0, 1)$ which is generated by a shift in time belongs to the value 18 in the three-dimensional case and therefore decreases 'more quickly' than in the two-dimensional case where this value is equal to 11. In the three-dimensional case there are, between the modes generated by shifts in space and the mode generated by a shift in time, still some items with higher angular mode numbers $m = \pm 2 \cdots \pm 10$ and $k = 0$.

CONCLUSION

The equation (1) describing the motion of an ice sheet under its own weight has a cylindrically symmetric similarity solution (2) (three-dimensional case) and a similarity solution (8) which is homogeneous in one horizontal direction (two-dimensional case). Its half-width (15) or (17) is a power function of the time where in the three-dimensional case the corresponding power exponent is lower than in the two-dimensional case. From both solutions the same time-independent surface profile (4) or (10) in a plane perpendicular to the bed and to the ice edge can be obtained by time-dependent rescalings of the space variables. In the perfect plasticity limit the three-dimensional or two-dimensional similarity solution yields Orowan's three-dimensional or two-dimensional solution, respectively.

Under the boundary condition of vanishing ice flux (38), the initial value problem of the equation of motion (36), which has been linearized in the deviations from the similarity solution, can be solved by expanding these deviations in terms of eigenfunctions of the linearized equation (57) or (58) and by determining the time evolution (60) of the amplitudes which occur as coefficients of the eigenfunctions in this expansion.

The symmetry properties of the eigenfunctions are denoted by the integer m. In the three-dimensional case $(m = 0, \pm 1, \cdots)$ the eigenfunctions belonging to m are determined by their angular dependence proportional to $e^{im\phi}$. In the two-dimensional case $(m = 0, 1)$, $m = 0$ denotes the symmetric and $m = 1$ the antisymmetric eigenfunctions under $x \rightarrow -x$. For every m, infinitely many eigenfunctions $\varepsilon_{m,k}(k = 0, 1, \cdots)$ (42) or (50) exist.

The eigenmodes can be ordered according to the relative rate of decrease $-\dot{a}_{m,k}/a_{m,k}$ of their amplitudes during the time evolution measured in units $\dot{R}/R$ which is the relative rate of increase of the cap's half-width (cf. (61) or (62)). In the three-dimensional as well as in the two-dimensional case, the lowest mode with $(m, k) = (0, 0)$ belongs to the value 0 and can be generated from the similarity solution by an infinitesimal shift in volume. Then follows the value 1, which belongs in the three-dimensional case to the two modes with $(m, k) = (\pm 1, 0)$ generated by shifts in two orthogonal horizontal directions and in the two-dimensional case to the mode with $(m, k) = (1, 0)$ generated by a shift in x-direction. For $n = 3$ the next value in the two-dimensional case is 11 and the corresponding mode with $(m, k) = (0, 1)$ can be generated by a time shift. In the three-dimensional case the mode which is generated by a time shift with $(m, k) = (0, 1)$ belongs to the value 18, and thus the corresponding amplitude decreases more quickly than in the two-dimensional case. However, in this case there are still the modes with $(m, k) = (\pm 2, 0) \cdots (\pm 10, 0)$ between the modes which are generated by space shifts and the mode which is generated by a time shift.

In the three-dimensional as well as in the two-dimensional case it follows from the solution (57) or (58) with (60) of the linearized equation (36) under the boundary condition of vanishing ice flux (38) that the similarity solution is asymptotically stable with respect to all perturbations of its initial value data which leave its volume invariant.

APPENDIX A

Consider the transformation

$$t = \sigma \qquad \phi = \chi \qquad \eta = (1 + \varepsilon(\sigma, \xi, \chi))\xi \tag{A1}$$

with the differential transformation matrix

$$\begin{bmatrix} \frac{\partial\sigma}{\partial t}, & \frac{\partial\sigma}{\partial\eta}, & \frac{\partial\sigma}{\partial\phi} \\ \frac{\partial\xi}{\partial t}, & \frac{\partial\xi}{\partial\eta}, & \frac{\partial\xi}{\partial\phi} \\ \frac{\partial\chi}{\partial t}, & \frac{\partial\chi}{\partial\eta}, & \frac{\partial\chi}{\partial\phi} \end{bmatrix} = \left(1 + \frac{\partial}{\partial\xi}(\xi\varepsilon)\right)^{-1}$$

$$\begin{bmatrix} 1 + \frac{\partial}{\partial\xi}(\xi\varepsilon), & 0, & 0 \\ -\xi\frac{\partial\varepsilon}{\partial\sigma}, & 1, & -\xi\frac{\partial\varepsilon}{\partial\chi} \\ 0, & 0, & 1 + \frac{\partial}{\partial\xi}(\xi\varepsilon) \end{bmatrix} \tag{A2}$$

The condition

$$\left|\frac{\partial}{\partial\xi}(\xi\varepsilon)\right| < 1 \tag{A3}$$

guarantees the regularity of (A2). From (A2) it follows up to first order in ε:

$$\frac{\partial}{\partial t} = \frac{\partial}{\partial\sigma} - \xi\frac{\partial\varepsilon}{\partial\sigma}\frac{\partial}{\partial\xi} \tag{A4}$$

$$\frac{\partial}{\partial\eta} = \left(1 - \frac{\partial}{\partial\xi}(\xi\varepsilon)\right)\frac{\partial}{\partial\xi} \tag{A5}$$

$$\frac{\partial}{\partial\phi} = -\xi\frac{\partial\varepsilon}{\partial\chi}\frac{\partial}{\partial\xi} + \frac{\partial}{\partial\chi} \tag{A6}$$

Inserting (A1), (A4), (A5), (A6), (3), (30), (32), and (33) in (1), one obtains the linearized equation of motion in ε

$$\begin{aligned}(5n+3)\sigma\frac{\partial}{\partial\sigma}(g(\xi) - \xi g'(\xi))\varepsilon \\ = -\frac{n}{\xi}\frac{\partial}{\partial\xi}\xi\left(\xi g(\xi)\varepsilon + \frac{\xi g(\xi)}{g'(\xi)}(g(\xi) - \xi g'(\xi))\frac{\partial\varepsilon}{\partial\xi}\right) \\ - \frac{g(\xi)(g(\xi) - \xi g'(\xi))}{\xi g'(\xi)}\frac{\partial^2\varepsilon}{\partial\chi^2}\end{aligned} \tag{A7}$$

The division by $(5n + 3)(g - \xi g')$ then yields (36) where $\partial/\partial\sigma$, $\partial/\partial\chi$ denote $\partial/\partial t$, $\partial/\partial\phi$, respectively, at fixed ξ.

APPENDIX B

To write (A7) in standard form, the transformations

$$z = \xi^{(1+n)/n} \qquad 0 < \xi < 1 \tag{A8}$$

$$\begin{aligned}\delta &= (g(\xi) - \xi g'(\xi))\varepsilon \\ &= \frac{n}{(2n+1)}\left(\frac{(2n+1)}{n} - z\right)(1-z)^{-(n+1)/(2n+1)}\varepsilon\end{aligned} \tag{A9}$$

are used. Replacing the operator $\sigma\,\partial/\partial\sigma$ by the spectral parameter μ;

$$\sigma\frac{\partial}{\partial\sigma} \to \mu \tag{A10}$$

writing δ as

$$\delta = \Delta(z)e^{im\chi} \tag{A11}$$

i.e.,

$$\frac{\partial^2\delta}{\partial\chi^2} = -m^2\delta \tag{A12}$$

and substituting (A8)–(A11) in (A7) yields

$$\begin{aligned}0 = \frac{\partial^2\Delta}{\partial z^2} + \left(\frac{2n}{(n+1)}\frac{1}{z} + \frac{(3n+2)}{(2n+1)}\frac{1}{(z-1)}\right)\frac{\partial\Delta}{\partial z} \\ + \left(-\frac{nm^2}{(n+1)^2}\frac{1}{z^2} - \frac{n(5n+3)}{(2n+1)(n+1)}\right. \\ \left.\cdot\left(\mu + \frac{2(n+1)}{(5n+3)}\right)\left(\frac{1}{z} - \frac{1}{(z-1)}\right)\right)\Delta\end{aligned} \tag{A13}$$

The condition (A3) is equivalent to

$$\begin{aligned}\left|\frac{(2n+1)}{n}\left(1 + \frac{(n+1)}{n}z\frac{\partial}{\partial z}\right)\left(\frac{(2n+1)}{n} - z\right)^{-1}\right. \\ \left.\cdot(1-z)^{(n+1)/(2n+1)}\Delta\right| < 1\end{aligned} \tag{A14}$$

The equation (A13) is Riemann's differential equation. Its complete set of solutions is denoted by the symbol [*Smirnow*, 1970]

$$\mathrm{P}\begin{bmatrix} 0 & 1 & \infty & \\ \alpha_1 & \beta_1 & \gamma_1 & z \\ \alpha_2 & \beta_2 & \gamma_2 & \end{bmatrix} \tag{A15}$$

where α_i, β_i, γ_i $(i = 1, 2)$ are the roots of the corresponding fundamental equation at $z = 0, 1, \infty$, respectively:

$$\alpha_{1,2} = \frac{1}{2(n+1)}(-n + 1 \pm ((n-1)^2 + 4nm^2)^{1/2}) \tag{A16}$$

$$\beta_1 = 0 \qquad \beta_2 = -\frac{(n+1)}{(2n+1)} \tag{A17}$$

$$\begin{aligned}\gamma_{1,2} = \frac{(5n^2+4n+1)}{2(n+1)(2n+1)} \pm \left(\frac{(3n^2-1)^2}{4(n+1)^2(2n+1)^2}\right. \\ \left. + \frac{nm^2}{(n+1)^2} - \frac{n(5n+3)\mu}{(n+1)(2n+1)}\right)^{1/2}\end{aligned} \tag{A18}$$

The set of solutions of (A13) can be represented in the neighborhood of $z = 0$ by

$$\Delta = c_1 z^{\alpha_1} w_1(z) + c_2 z^{\alpha_2} w_2(z) \tag{A19}$$

with arbitrary constants c_1, c_2 and functions $w_1(z)$, $w_2(z)$ which are analytic in the neighborhood of $z = 0$ and nonvanishing at $z = 0$:

$$w_1(0) \neq 0 \qquad w_2(0) \neq 0 \tag{A20}$$

A similar representation exists in the neighborhood of $z = 1$:

$$\Delta = c_3(1-z)^{\beta_1} w_3(z) + c_4(1-z)^{\beta_2} w_4(z) \tag{A21}$$

$$w_3(1) \neq 0 \qquad w_4(1) \neq 0 \tag{A22}$$

From (A14), (A17), (A21), and (A22) it follows that

$$c_3 = 0 \tag{A23}$$

and from (A16), (A19), and (A20) that

$$c_2 = 0 \tag{A24}$$

Thus $(1-z)^{-\beta_2}z^{-\alpha_1}\Delta$ is analytic in the entire complex z plane. The special function of the set [*Abramowitz and Stegun*, 1970]

$$(1-z)^{-\beta_2}z^{-\alpha_1}P\begin{bmatrix}0 & 1 & \infty & \\ \alpha_1 & \beta_1 & \gamma_1 & z\\ \alpha_2 & \beta_2 & \gamma_2 & \end{bmatrix} = P\begin{bmatrix}0 & 1 & \infty & \\ 0 & \beta_1-\beta_2 & \gamma_1+\alpha_1+\beta_2 & z\\ \alpha_2-\alpha_1 & 0 & \gamma_2+\alpha_1+\beta_2 & \end{bmatrix} \quad \text{(A25)}$$

which is analytic in the entire z plane is the hypergeometric function $F(a, b, c; z)$ where

$$a, b = \gamma_{1,2} + \alpha_1 + \beta_2 \qquad c = 1 + \alpha_1 - \alpha_2 \quad \text{(A26)}$$

and a or b must be a nonpositive integer $-k$ which implies (cf. (A16)–(A18), (A26))

$$b = -k \quad \text{(A27)}$$

$$a = k + \frac{n}{(2n+1)} + \frac{1}{(n+1)}\left((n-1)^2 + 4nm^2\right)^{1/2} \quad \text{(A28)}$$

$$c = 1 + \frac{1}{(n+1)}\left((n-1)^2 + 4nm^2\right)^{1/2} \quad \text{(A29)}$$

Using (A16)–(A18), (A26)–(A29) yield the eigenvalues $\mu_{m,k}$ (41).

Appendix C

In the following it is shown that the condition $c_3 = 0$ (A23) which is equivalent to (37) is also equivalent to (38). Using (3), (30) yields for the flux $\mathbf{q}$

$$\mathbf{q} = -\nabla h|\nabla h|^{n-1}h^{n+2} = -f^{5n+4}(aV)^{(n+2)/3}\left(\mathbf{e}_\rho G_\eta + \mathbf{e}_\phi \frac{G_\phi}{\eta}\right)\left({G_\eta}^2 + \frac{{G_\phi}^2}{\eta^2}\right)^{(n-1)/2} G^{n+2} \quad \text{(A30)}$$

where $(\mathbf{e}_\rho, \mathbf{e}_\phi)$ is the orthonormal system which belongs to cylindrical coordinates. Substituting (33), (A1), (A5), (A6), (A8), (A9), and (A11) in (A30) and expanding its radial and angular part up to first order in δ yields

$$G_\eta\left({G_\eta}^2 + \frac{{G_\phi}^2}{\eta^2}\right)^{(n-1)/2} G^{n+2} = -\left(\frac{n+1}{2n+1}\right)^n z^{n/(1+n)}(1-z)^{n/(2n+1)} - \delta\left(\frac{n+1}{2n+1}\right)^n \frac{1}{n} z^{n/(n+1)}\left(\frac{(2n+1}{n} - z\right)^{-1} \cdot \left((n+3)(2n+1) - (n^2+5n+2)z\right) + \frac{\partial\delta}{\partial z}\left(\frac{n+1}{2n+1}\right)^n (2n+1)z^{n/(n+1)}(1-z) \quad \text{(A31)}$$

$$\frac{G_\phi}{\eta}\left({G_\eta}^2 + \frac{{G_\phi}^2}{\eta^2}\right)^{(n-1)/2} G^{n+2} = \mathrm{im}\delta\left(\frac{n+1}{2n+1}\right)^{n-1} z^{-1/(n+1)}(1-z) \quad \text{(A32)}$$

In the vicinity of the edge $z = 1$, δ is given by (cf. (A11), (A17), and (A21))

$$\delta = (c_3 w_3(z) + c_4 w_4(z)(1-z)^{-(n+1)/(2n+1)})e^{\mathrm{im}\chi} \quad \text{(A33)}$$

Substituting (A33) into (A31) and (A32) yields

$$G_\eta\left({G_\eta}^2 + \frac{{G_\phi}^2}{\eta^2}\right)^{(n-1)/2} G^{n+2} = -\left(\frac{n+1}{2n+1}\right)^n z^{n/(n+1)}(1-z)^{n/(2n+1)} + \left(\frac{n+1}{2n+1}\right)^n e^{\mathrm{im}\chi} z^{n/(n+1)}\left(\frac{(2n+1)}{n} - z\right)^{-1} \cdot \left[-c_3 w_3(z)\frac{1}{n}\left((n+3)(2n+1) - z(n^2+5n+2)\right) + (2n+1)c_3 w_3'(z)(1-z)\left(\frac{(2n+1)}{n} - z\right) + (1-z)^{n/(2n+1)}\left((2n+1)\left(\frac{(2n+1}{n} - z\right) \cdot c_4 w_4'(z) - \frac{2(2n+1)}{n} c_4 w_4(z)\right)\right] \quad \text{(A34)}$$

$$\frac{G_\phi}{\eta}\left({G_\eta}^2 + \frac{{G_\phi}^2}{\eta^2}\right)^{(n-1)/2} G^{n+2} = ime^{\mathrm{im}\chi}\left(\frac{n+1}{2n+1}\right)^{n-1} z^{-1/(n+1)} \cdot \left((1-z)c_3 w_3(z) + (1-z)^{n/(2n+1)} c_4 w_4(z)\right) \quad \text{(A35)}$$

The angular part (A35) vanishes at the edge $z = 1$ in any case, but the radial part (A34), due to (A22), if and only if $c_3 = 0$.

Appendix D

Using the orthogonality relations [*Abramowitz and Stegun*, 1970]

$$\int_0^1 dz\, w_m(z) u_{m,k}(z) u_{m,l}(z) = \delta_{k,l} \quad \text{(A36)}$$

for the polynomials $u_{m,k}(z)$, (45) or (53) with the weight function

$$w_m(z) = (1-z)^{p_m - q_m} z^{q_m - 1} \quad \text{(A37)}$$

one obtains the inverse relation to (57):

$$a_{m,k}(t) = \frac{1}{2\pi}\int_0^{2\pi} d\phi \int_0^1 dz\, e^{-\mathrm{im}\phi} w_m(z) f_m^{-1}(z) \cdot u_{m,k}(z)\varepsilon(t, \xi, \phi) \quad \text{(A38)}$$

and to (58):

$$a_{m,k}(t) = \int_{\substack{0\\ \xi>0}}^1 dz\, w_m(z) f_m^{-1}(z) u_{m,k}(z) \cdot \frac{1}{2}\left(\varepsilon(t, \xi) + (-1)^m \varepsilon(t, -\xi)\right) \quad \text{(A39)}$$

Acknowledgments. I thank K. Hasselmann for many discussions.

References

Abramowitz, M., and I. A. Stegun (eds.), *Handbook of Mathematical Functions*, pp. 556, 564, 773–775, Dover, New York, 1970.

Halfar, P., On the dynamics of the ice sheets, *J. Geophys. Res.*, *86*, 11065, 1981.

Mahaffy, M. W., A three dimensional numerical model of ice sheets:

Tests on the Barnes ice cap, Northwest Territories, *J. Geophys. Res.*, *81*, 1059, 1976.
Nye, J. F., The mechanics of glacier flow, *J. Glaciol.*, *2*, 82, 1952.
Nye, J. F., The distribution of stress and velocity in glaciers and ice sheets, *Proc. R. Soc. Ser. A*, *239*, 113, 1957.
Smirnow, W. I., *Lehrgang der Höheren Mathematik*, vol. III/2, p. 315, VEB Deutscher Verlag der Wissenshaften, Berlin, 1970.
Weertman, J., Rate of growth and shrinkage of nonequilibrium ice sheets, *J. Glaciol.*, *5*, 145, 1964.

(Received January 18, 1982;
revised January 17, 1983;
accepted February 22, 1983.)